

# Factors affect bond of fiber-reinforced polymer laminates to concrete

Magda I. Mousa

Dr.magdashehata@yahoo.com, Structural Engineering Department, Faculty of Eng.  
El-Mansoura University, Egypt

**Abstract.** *Fiber reinforced polymer (FRP) sheet is one of the most popular method used that externally bonded for flexural retrofit of concrete member. However, the problem of dismantling of the fiber mostly happened and causes a strength reduction of the retrofitted member.*

*In this study, a total of 17 plain concrete beams were studied experimentally and analyzed. Three groups of different concrete strength (33.5, 40.7 and 67 MPa) were used to cast the tested beams. The beam is simply supported and has a span of 1110 mm and 120 × 250 mm cross-section. Carbon fiber reinforced polymer (CFRP) sheet of unidirectional type bonded at the tension surface of the beams. The factors affecting the bond between CFRP sheets and concrete like; length of bonded surface, compressive strength of concrete, number of plies of CFRP (stiffness), and the roughness of concrete surface were studied.*

*All specimens were subjected to a four-point bending test under load control while cracking load, mid-span deflection, and strain distribution along the bonded length of CFRP sheet and failure mode were recorded up to failure.*

*Results indicated that the bond length affects significantly the average bond stress of the strengthened beams (shear bonding stress due to flexural loading). The bonding distribution along the CFRP sheet due to flexural loading tended to be linear when the applied load close to ultimate load.*

**Keywords:** *Composite; Externally Bonded Retrofit; CFRP sheet; Bond length; Flexure.*

## I. INTRODUCTION

Externally bonded of fiber reinforced polymer (FRP) plates or sheets has arose as a popular method for the strengthening and retrofitting of reinforced concrete (RC) structures [1]–[6]. The bond is the means for the transfer of stress between the concrete and FRP in order to achieve composite action. Therefore, for the safe and economical design of externally bonded FRP systems, a sound understanding of the behaviour of FRP to- concrete interfaces needs more investigation.

The use of carbon fiber-reinforced polymers (CFRP) can now be considered common practice in the field of strengthening and rehabilitation of reinforced concrete structures either in shear or in flexure. The use of CFRP in strengthening structural concrete members provides additional flexural or shear

reinforcement, the reliability for this material application depends on how well they are bonded and can transfer stress from the concrete component to CFRP laminate [7].

The success of externally reinforcing members depends mainly on the integrity of the bond between the FRP and the original material. Primary considerations include surface preparation, epoxy quality and laminate application: a successful bond depends heavily on the quality of the workmanship as depends on the reliability of the material.

Two types of failure modes of FRP strengthened beams are Possible; the first type of failure includes the common failure modes such as, concrete crushing and FRP rupture based on complete composite action, the second type of failure is a precocious failure without reaching to full composite action at failure. This type of failure includes: end cover separation, end interfacial delamination, flexural crack induced debonding and shear crack induced debonding.

Several studies were performed to identify methods to overcome of precocious failure with the aim of improving the load capacity and ductility of RC beams. Researchers studied different techniques to ensure full composite action like the use of end anchorage techniques. The anchorage techniques used such as U-straps, L-shape jackets, and steel clamps for preventing premature failure of RC beams strengthened with CFRP [6], [8]–[15].

Several studies were conducted to study the behaviour of retrofitted beams and analyzed the various parameters influencing their behaviour and affect the bond strength between beams and the materials used in retrofitting [3], [16]–[18].

B. Miller and A.Nanni [2] conducted an experimental program aimed at investigating the strain distribution between Carbon Fiber Reinforced Polymer (CFRP) sheets and concrete. The effects of bonded length, concrete strength, and number of plies (stiffness) of CFRP were investigated. From the results, he proposed an equation for calculating the effective FRP ultimate strain.

H. Toutanji L. Zhao, Y. Zhang [1], carried out the test of eight RC beams and analyzed: one control beam and seven beams reinforced with three to six layers of carbon fiber

sheets bonded by an inorganic epoxy. All beams were subjected to a four-point bending test under load control while load, deflection, mid-span strain and failure mode were recorded up to failure. They found that the load carrying capacity increases with the increase of carbon fiber (CFRP) sheet layers up to 170.2% of the control beam strength. For beams with three and four of CFRP layers failed by rupture of fiber, while beams with five and six layers of FRP reinforcement failed by FRP delamination. The ductility of the CFRP strengthened beams is greatly reduced compared to the control beam.

The interaction between CFRP sheet and the concrete surface is an important factor to achieve full mechanical capacity of the flexural beams. The premature failure which limited the flexural capacity of the beams, may occur when the bond stress in the CFRP exceed the bonding capacity. Different studies have been conducted to investigate the bonding strength of CFRP sheet.

D.U. Choi, T. H. K. Kang, S. S. Ha, K. H. Kim, and W. Kim [19] conducted a bond test of hybrid FRP sheet under direct tensile loading using double face shear tests specimens. They concluded that the bonding stress estimated through a direct test cannot be applied directly in designing of the flexural beams.

R. Djamaluddin, M. A. Sultan, R. Irmawati, and H. Shinichi [20] presented the results of experimental investigation of the bonding behaviour on the strengthened concrete beams due to flexural loadings. The concrete beams used were strengthened with GFRP sheet on extreme tension surface. Their results indicated that the bonding distribution along the GFRP sheet due to flexural loading tended to be non-linear. They found that the bond stress due to flexural loading was lower than the direct shear bond stress. Further study is required to clarify the bond behaviour of CFRP sheet on the strengthen beams under flexural loadings.

## II. OBJECTIVES

The external retrofitting by attaching or wrapping FRP shaped sheet or plate, to concrete surface with epoxy is the most general method which have been used up to now in many structures retrofitting. The main objective of this research was to study the factors affecting the bond between CFRP sheets and concrete and to observe the bonding behaviour of CFRP sheet on concrete beams under flexural loading. The factors that were studied were; bonded length, compressive strength of concrete, number of plies (stiffness) of FRP and surface texture of concrete (roughness). This investigation is carried out in terms of mode of failure, cracking and ultimate loads, mid-span deflection, strain distribution along the bonded length and bond stress calculation.

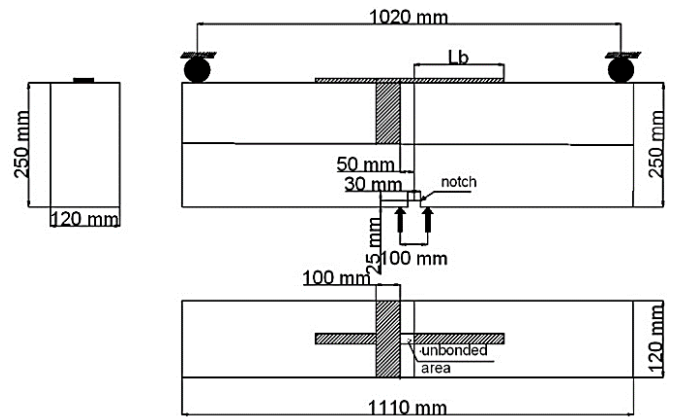


Fig. 1 Details of test specimen.

## III. EXPERIMENTAL PROGRAM

### A. Description and production of the tested beams

Three groups of plain concrete beams were casted using different compressive strength concrete. The first group consists of six beams with average compressive 28-days cubic strength of 33.5MPa, whilst the second group consist of 5 beams of 42MPa, and the third group of 6 beams with concrete strength of 67 MPa.

The parameters considered were, the bonded length (100mm, 150mm, 225mm, and 300mm), width of the strip, number of CFRP sheet plies, and the surface preparation (smooth, rough). The beams were 1110mm long, 120mm wide and 250mm deep. In the middle of the beam, a notch at the top during casting (25 mm depth and 30 mm width) and a saw cut (25 mm depth) at the bottom after the specimens were cured, was created to let a crack pass between the saw cut of the beam and the notch.

The specimens were de-moulded after 24 h and then were covered with wet burlap and plastic at room temperature for 28 days curing time. After 28-days curing, 4 cubes of 150 mm × 150 mm × 150 mm were tested in compression, 4 cylinders (150 mm diameter × 300 mm high) were tested in splitting and 4 prism specimens of 100 mm × 100 mm × 500 mm were tested in flexure for each mix to determine the mix properties. After the specimens had cured, the beam bottom surface where the CFRP sheet had to be applied was uniformly abraded by using a disc sander, and removing the dust and any loose particles generated by surface abrading using an air blower and some of specimens were roughened using a hammer and chisel to remove the top mortar and until the aggregate was appeared (~ 2mm depth roughness). Characteristics of all specimens are shown in Table I.

Table I Specimen details.

Group	Specimen designation <sup>a</sup>	Bond length, L <sub>b</sub> (mm)	CFRP width (mm)	No. of CFRP Plies	Surface texture <sup>b</sup>	No. of strain gages
Group I	N-1-10	100	50	1	S	3
	N-1-15	150	50	1	S	4
	N-1-22	220	50	1	S	4
	N-1-30	300	50	1	S	--
	N'-1-15	150	100	1	S	--
	N''-1-15	150	50	1	R	--
Group II	M-1-15	150	50	1	S	--
	M-2-15	150	50	2	S	4
	M-1-22	220	50	1	S	--
	M-2-22	220	50	2	S	4
	M-2-30	300	50	2	S	--
Group III	H-1-10	100	50	1	S	3
	H-1-15	150	50	1	S	4
	H-1-22	220	50	1	S	5
	H-1-30	300	50	1	S	5
	H'-1-15	150	100	1	S	4
	H''-1-15	150	50	1	R	4

Specimen designation<sup>a</sup> code: M-Y-P

M=N for normal strength concrete,

M for medium strength concrete,

H for high strength concrete,

M' = specimen with CFRP sheet width of 50mm,

M'' = specimen with roughen surface.

Y = No. of CFRP layers. P = bonded length in mm.

Surface texture<sup>b</sup>: S = smooth and R= rough.

A composite system consisting of a unidirectional carbon fiber fabric and epoxy based impregnating resin of two compounds A (white) and B (Grey) was used to carry this experimental study. At the beginning the material of each component mixes separately. Then added component B in component A with ratio 1:4 by weight and ideally mixed using the special Sika spatula. The two components were

stirred with an electric mixer for approximately 3 min. until all the coloured streaks have disappeared. Then the whole mix stirred again for 1 min at low speed to keep air entrainment at a minimum. The mixed resin was applied to the prepared substrate in the tension surface using brush in a suitable quantity (in average around 1kg/m<sup>2</sup>), depending on roughness of substrate. The CFRP sheets were cut into strips 50 mm wide and in some cases into 100 mm wide. Figure 1 shows the dimensions and the details of the tested specimen. The CFRP sheet was placed onto the resin coating in the required place and direction (Fig. 1). A strip of CFRP sheet (of a 50mm width or 100mm) was bonded to the tension surface of the beam. A 50mm on each side of the beam centre was left unbonded to ensure that no cracking would occur in the bonded area. A transverse sheet was placed over one side of the bonded strip thereby the failure could occur at the other side.

The plastic laminating roller was applied on the fabric to eliminate any air and until the resin is squeezed out through the fabric. In case of application two plies or the CFRP transverse sheet, more coating of resin would put and the fiber strip placed in similar way. The resin was allowed to cure for 10 days in the laboratory prior to testing.

The beams were turned upside down before being placed on the test frame to follow the failure stage and accurately record the mode of failure. The beams loaded in four-point bending as shown in Fig.2 using a hydraulic jack to apply the static load with an increment of 5 kN until failure.



Fig. 2 Test set-up.

The clear span of the beam was 1020mm and the two loading points were 100mm apart around the beam's mid-span. A series of electrical resistance strain gauges (with 120 Ω resistances) were attached along the length of the CFRP sheet to measure the strain in the fiber during the test. Three to five strains were placed along the centreline of the fiber

sheet according to the fiber length, one strain gages was attached at 50 mm far from the centre of the beam. The others strains placed each 50mm distance.

**B. Materials and Mix Proportions**

The constituent materials of the mix are CEM I 42.5N Portland cement, natural sand, gravel, tap water as well as silica fume and high-range water-reducing admixture in high strength mix. The fine aggregate was natural siliceous sand with 4.75 mm maximum particle size and with specific gravity and volumetric weight of 2.65 and 1600 kg/m<sup>3</sup>, respectively. The coarse aggregate was gravel of two sizes (10 mm and 20 mm), with specific gravity 2.7, and volumetric weight of 1700 kg/m<sup>3</sup>. The Silica fume was a very fine by product powder obtained as a fume from the foundry process in the Egyptian company of Iron Foundries. The Silica fume used contains 95% of SiO<sub>2</sub>. The high-range water-reducing admixture used was the Polynaphthalene Sulphonate type. The material properties of a unidirectional CFRP sheet and the resin used in this research are illustrated in Table II and III. The proportions and the mechanical properties of the concrete mixes which have used for specimens' preparation are given in Table IV.

**Table II Material properties of CFRP-sheet**

Fiber type	Thickness (mm)	Tensile strength (MPa)	Tensile E Modulus (MPa)
Sika Wrap Hex-230 C	0.13	3500	230,000

**Table III Material properties of resin.**

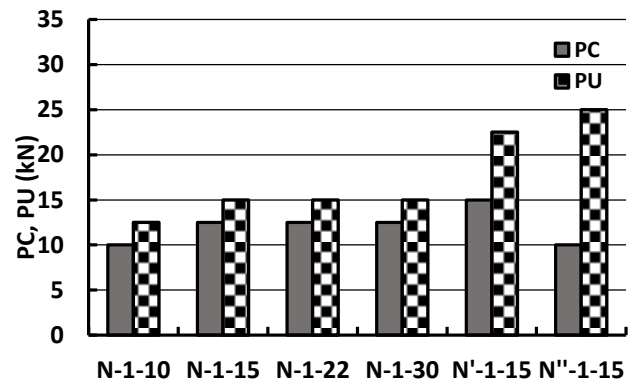
Resin type	Mixing ratio	Tensile strength (MPa)	Flexural E Modulus (MPa)
Sikadur -330	A:B= 4:1 by weight	30.0	3800

**IV. TEST RESULTS AND DISCUSSION**

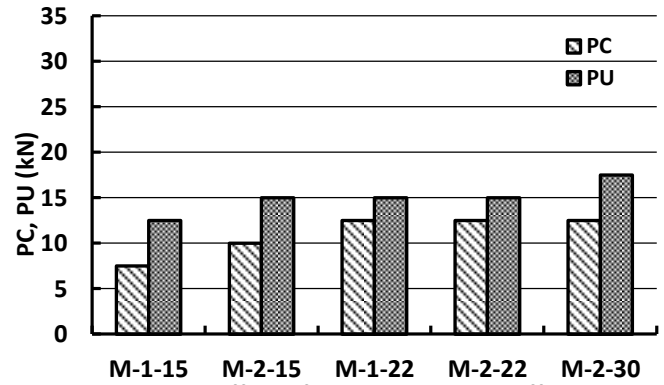
**A. Cracking load, ultimate load and failure mode**

Table V shows a summary of the flexural behaviour of all test beams in terms of cracking load, flexural ultimate load, ultimate mid-span deflection and failure mode. The bonded length of the CFRP sheet was found to have a determined effect on the cracking and the ultimate load of the specimen, Figs 3-5. In normal strength concrete (group I), the cracking load and the ultimate load increased with increasing the bonded length up to a certain limit. The increase was up to bond length ( $L_b$ ) of 150mm; with increasing about to 25% and 20% for  $P_C$  and  $P_U$ , respectively,

compared with  $L_b$  of 100mm, this implies that an effective bond length exists. While, in high strength concrete (HSC) the increase was continued up to  $L_b$  of 300mm for both  $P_C$  and  $P_U$ ; with maximum increase about 50% and 47%, respectively, compared with specimens of  $L_b = 100$ mm. The mode of failure was by debonding in NSC specimen with  $L_b = 100$ mm and up to  $L_b = 150$ mm in HSC specimens. Whilst, the failure was by fiber rupture started of  $L_b = 150$ mm in NSC and of  $L_b = 220$ mm in HSC.



**Fig. 3 Effect of CFRP length, width, and roughness surface on cracking and ultimate loads (group I).**



**Fig. 4 Effect of CFRP length and stiffness on cracking and ultimate loads (group II).**

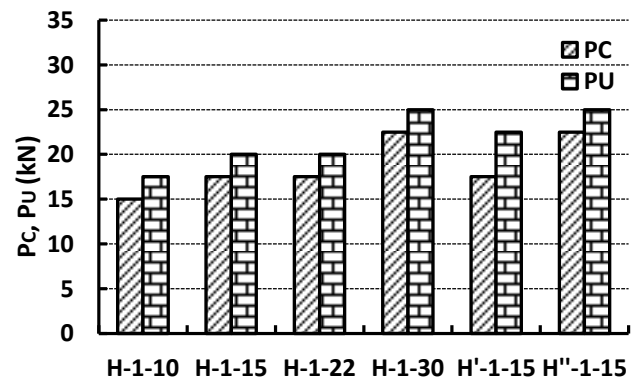


**Fig. 5 Effect of CFRP length, width, and roughness surface on cracking and ultimate loads (group III).**

Table IV Concrete Mix Proportion and its Properties

Mix designation	Mix proportion(Kg/m <sup>3</sup> )						Superplasticizer (SP. %)
	Cement content	Sand content	Gravel content		Water content	Silica fume (SF)	
			Max. Size 10mm	Max. Size 20mm			
N	350	680	–	1360	138.5	–	–
M	500	659	408	815	110	–	25
H	500	620	411	824	126.5	75	14.4 (2.5%)
Mix properties							
Mix designation	Comp. Strength $f_{cu}$ (MPa)		Flexural Strength $f_r$ (MPa)		Split. Tens. Strength $f_{sp}$ (MPa)		
N	33.5		3.95		3.25		
M	40.3		4.8		3.07		
H	67.0		10.6		5.10		

TABLE V: Summary of Cracking Load, Ultimate Load and Ultimate Deflection

Group	Specimen designation	Cracking load, $P_C$ (kN)	Ultimate load, $P_U$ (kN)	Ultimate deflection $\Delta_U$ (mm)	Tensile on fiber $T_f$ (kN)	Average Bond strength $f_{br}$ (MPa)	Failure <sup>c</sup> pattern
Group I	N-1-10	10.0	12.5	3.0	16.74	3.35	DL
	N-1-15	12.5	15.0	3.0	16.7	2.22	FR
	N-1-22	12.5	15.0	2.9	16.54	1.50	FR
	N-1-30	12.5	15.0	2.8	--	--	FR
	N'-1-15	15.0	22.5	3.11	--	--	DL
	N''-1-15	10.0	25.0	2.96	--	--	FR
Group II	M-1-15	7.5	12.5	2.5	--	--	FR
	M-2-15	10.0	15.0	1.95	16.85	2.25	DL
	M-1-22	12.5	15.0	3.1	--	--	FR
	M-2-22	12.5	15.0	2.25	--	--	DL
	M-2-30	12.5	17.5	1.85	--	--	DL
Group III	H-1-10	15.0	17.0	2.0	19.07	3.81	DL
	H-1-15	17.5	20.0	2.02	22.44	2.99	DL
	H-1-22	20.0	22.5	2.00	25.82	2.35	FR
	H-1-30	22.5	25.0	1.25	23.07	1.54	FR
	H'-1-15	17.5	22.5	1.75	25.87	1.73	FR
	H''-1-15	20.0	25.0	2.15	23.07	3.08	FR

Failure pattern<sup>c</sup>: D = depending of CFRP strip and FR= Fiber rupture.

The  $P_C$  and  $P_U$  increased by 20% and 50% due to increasing the CFRP sheet width for group I specimens (NSC) whilst, for group III (HSC) the increase was only 12.5% in  $P_U$ . The roughness of the concrete surface was affected significantly on the ultimate load particularly in normal strength concrete (NSC), with about 67% increase whereas with 25% in HSC. The improved surface preparation by roughening and increasing the fiber sheet width were found to improve the bond strength to the point where failure occurred by fiber rupture in HSC.

The number of plies (stiffness) of CFRP sheet had a considerable influence on the bond behaviour, all the specimens with double layers of CFRP sheet exhibited debonding failure whilst fiber rupture occurred in the one layer specimens of medium strength concrete (group II). The  $P_C$  and  $P_U$  increased by 33% and 20% due to increasing the stiffness of CFRP sheet (M-2-15). However, for specimen with  $L_b = 220\text{mm}$  (M-2-22) the  $P_C$  and  $P_U$  had not record any change.

The photographs shown in Fig.6a, 6b, and 6c represent the failure mode of specimens. The failure was initiated by the flexural cracks occurred at the mid-span of the beams. Increasing of the applied load caused the increase in bonding stress at the crack edge. Once the bonding stress exceeded the bonding capacity, the beam failed due to delaminating of the GFRP sheet. The delaminating started from the crack edge simultaneously to the end of the CFRP sheet. While whenever the bond stress is more than the allowable fiber tensile strength, the rupture of the fiber may be occur.

**B. Load vs. deflection at mid-span**

Figs. 7-9 show the load versus deflection at mid-span for all studied beams. The load–deflection curves can be classified to two distinct zones; the first zone is the initial part of the curve up to almost the cracking point, the post-cracking zone, continued up to failure. Both the zones were relatively linear. At the initial stage the beams stiffness showed almost identical behaviour at low level of loading before the cracking stage particularly in NSC group, as this stage is controlled mainly by the concrete tensile strength. The second zone, showed a distinct behaviour in the different beams. From the figures, it is obvious that the increase of bonded length increase the stiffness of the beam particularly in HSC (by comparing specimens H-1-15, H-1-22, and H-1-30 with H-1-10). The ultimate deflection of the beams N-1-10 and N-1-15 was identical and N-1-22, N-1-30 were slightly less than N-1-10 by about 3.3% and 6.7%, respectively.

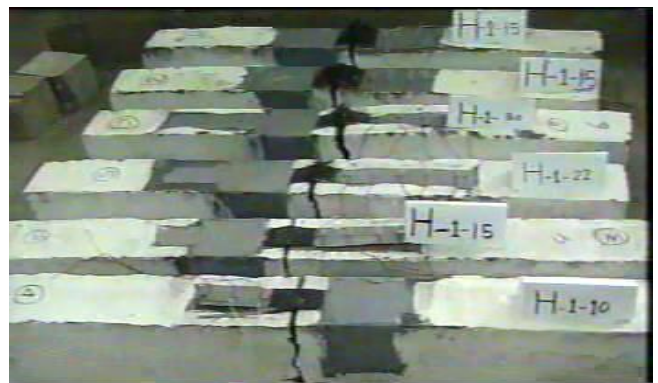
Regarding to HSC group,  $\Delta_U$  decreased in the beam H-1-30 by about 38% compared with H-1-10 specimen. Whilst the beam H-1-15 and H-1-22 recorded similar ultimate deflection compared to H-1-10 specimen.



(a)



(b)



(c)

**Fig. 6. Photographs of the failed specimens in different groups.**

Increasing the CFRP sheet width (N'-1-15, H'-1-15) and roughing the concrete surface (N''-1-15, H''-1-15) in both NSC and HSC groups showed a significant and a distinct behaviour. In these cases the stiffness, particularly after cracking stage, was increased. The ultimate deflection ( $\Delta_U$ ) was increased in H''-1-15 specimen with about 6.4% whilst,  $\Delta_U$  decreased with 13% due to increasing the fiber width from 50 mm to 100 mm, H'-1-15. However, the specimens N'-1-15 and N''-1-15 relatively did not alter the ultimate deflection, Fig. 7.

On the other hand, with increasing the number of CFRP sheet layers on the beams the stiffness was increased in both the zones of the load-deflection curve, before and after cracking, as shown in Fig. 8. In addition, the ultimate deflection in beams that have two-ply of CFRP sheet decreased compared with the beams which have one ply. The reduction in the ultimate deflection was 22% and 27.4% in beams M-2-15 and M-2-22, respectively, compared with the corresponding beams M-1-15 and M-1-22. This reduction in ultimate deflection refers to low ductility and indicates that the addition of CFRP sheet layers greatly reduces the deformability at the ultimate stage of loading.

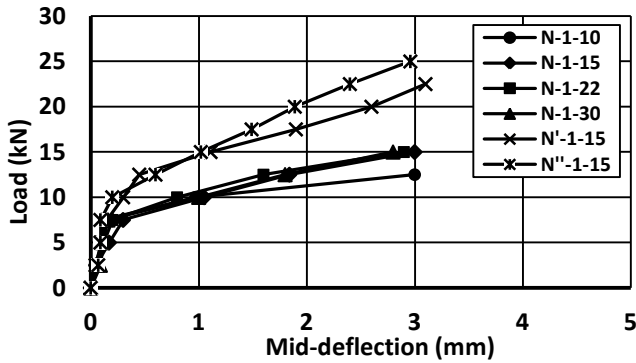


Fig. 7. Load - mid-deflection relationship (group I).

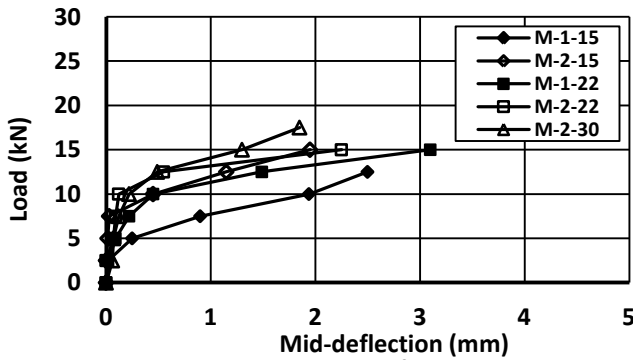


Fig. 8. Load - mid-span deflection relationship (group II).

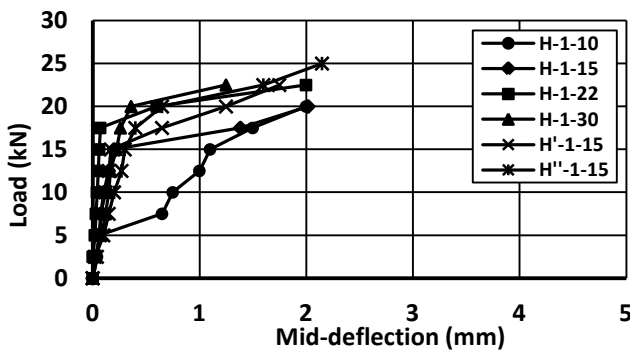


Fig. 9. Load - mid-span deflection relationship (group III).

### C. Bond strength evaluation

The bonding behaviour of CFRP sheet attached at the extreme tensile surface of the beams under flexural loading could be explained as follow:

At the beginning of loading, the beam was uncracked and the concrete section resisted both the compression and the tension stresses. Once the concrete cracks, all the tension stresses was resisted by the CFRP sheet. Further loading caused crack propagation and the crack width increased. As the results the compression stress increased and equilibrates the tensile stress produced at the CFRP sheet. The flexural strain and stress diagram and the flexural bonding stress produced on CFRP sheet shown in Fig. 10.

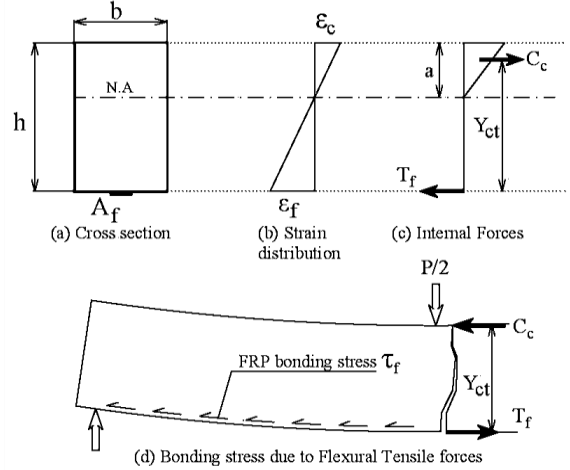


Fig. 10. Bonding stress in flexural beam.

It was observed for all the tested beams, that the concrete was not crushed in compression zone (tension failure). So, the strain and stress distribution may be assumed in elastic relationship as shown ( $\epsilon_c \leq 0.002$ ). The  $M_u$  of the beam was calculated from the force  $C_c$  resisted by concrete or the tension force on CFRP sheet multiplied by the arm between them,  $y_{ct}$ , as follow.

$$M_u = T_f \times y_{ct} = C_c \times y_{ct} \quad (1)$$

$$y_{ct} = \left( h - \frac{1}{3} a \right) \quad (2)$$

$$a = \frac{\epsilon_c}{\epsilon_f + \epsilon_c} \quad (3)$$

Where,  $\epsilon_c$  is the concrete strain and may be assumed to = 0.002,  $h$  = the beam height, and  $\epsilon_f$  = the experimental strain in CFRP sheet.

The tensile force of CFRP sheet may be estimated from equation (4) as follow.

$$T_f = \frac{M_u}{\left( h + \frac{1}{3} a \right)} \quad (4)$$

The average bonding stress (shear bonding stress) on the CFRP sheet may be simply estimated by using equation (5).

$$\tau_f = \frac{T_f}{A_{bf}} \quad (5)$$

where,  $A_{bf}$  represent the bonding area of the CFRP sheet. The calculation of the average bonding stress on different studied beams is shown in Table V.

The results of calculated average bonding stress ( $\tau_f$ ) indicated that the bonding stress on the CFRP sheet reduced with increasing the bonding length ( $L_b$ ). In normal strength concrete, increasing the bond length from 100mm to 220mm reduced the bond stress significantly with about 55%. Whilst, in HSC the reduction was about 60% with increasing the  $L_b$  from 100mm to 300mm in HSC group. However, doubling the width of CFRP sheet from 50mm to 100mm caused a reduction by about 55% in the average bond stress of HSC due to flexural loading. On the other hand, the results show limited effect of surface roughness on the average bond strength in HSC (compare the specimen H`-1-15 to H-1-15).

#### D. Load vs. strain

Figs. 11-18 show the tension strain distribution at a distance of 50 mm from the center and along to the far end of the bond length of fiber sheet that represents the bond stress distribution. These curves illustrate the strain as a function of the distance of the strain gage and each curve is plotted for a given load level. The strain gauges recorded increase in the values as the load increase and as the distance from the beam center decreased. At beginning of loading the curves show nonlinear shape and with increasing the load the curves become almost linear as shown in Figures. In NSC the maximum strain increased with increasing the bonded length, whilst in HSC exhibited almost same value even in specimens with CFRP sheet of width 100mm or with rough surface. The maximum values of strain of NSC specimen were higher compare with HSC specimen.

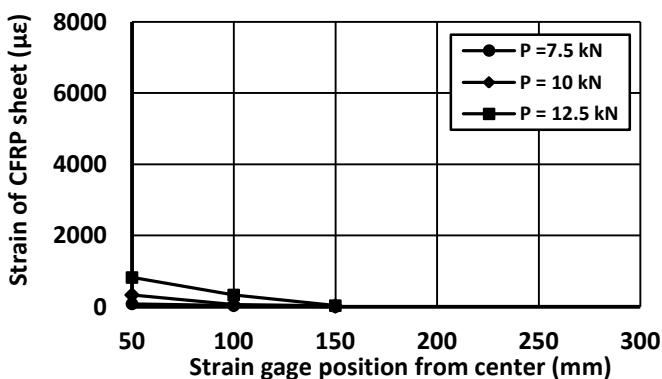


Fig. 11. Strain distribution of N-1-10 specimen.

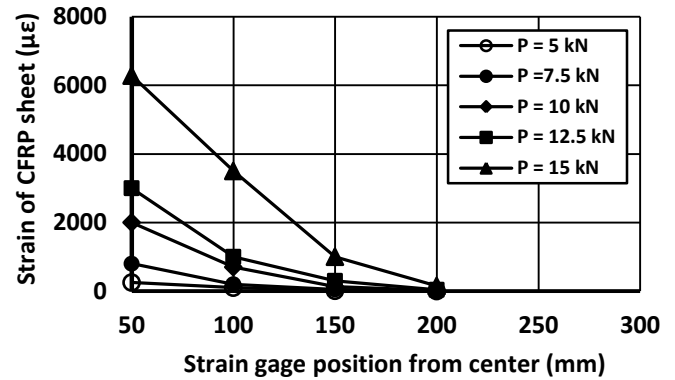


Fig. 12. Strain distribution of N-1-15 specimen.

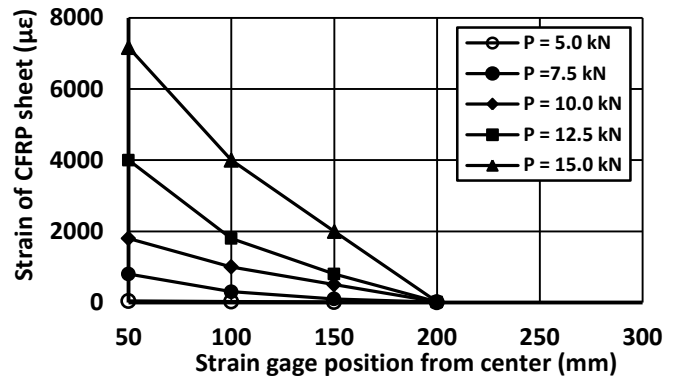


Fig. 13. Strain distribution of N-1-22 specimen.

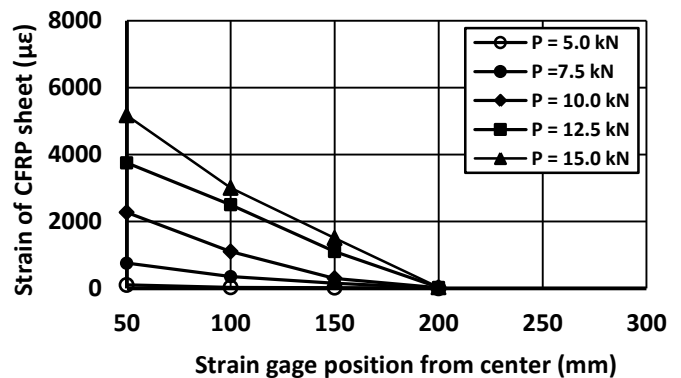


Fig. 14. Strain distribution of M-2-22 specimen.

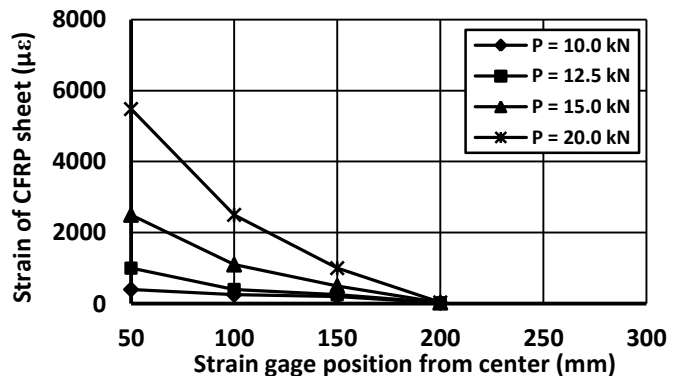


Fig. 15. Strain distribution of H-1-15 specimen.

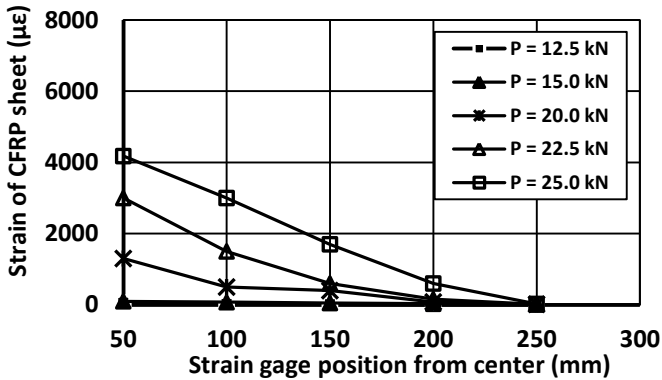


Fig. 16. Strain distribution of H-1-30 specimen.

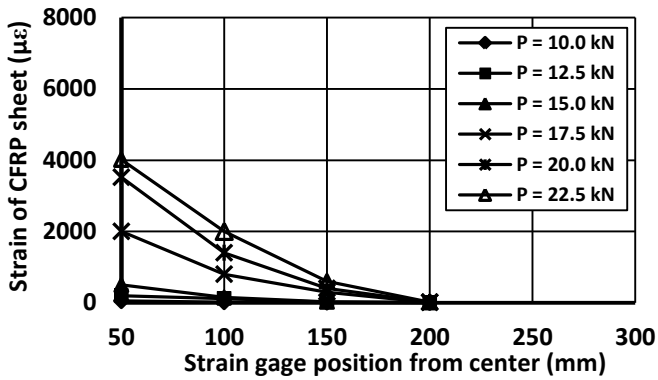


Fig. 17. Strain distribution of H'-1-15 specimen.

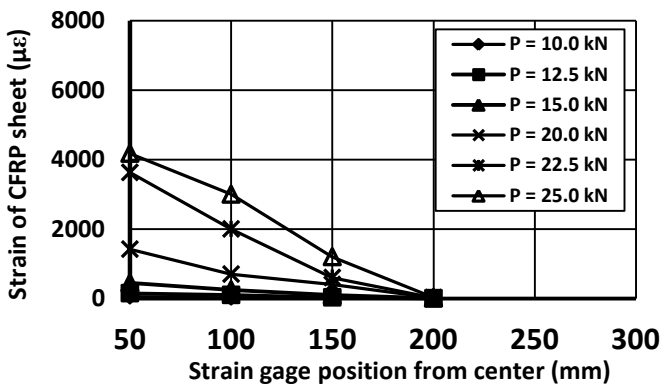


Fig. 18. Strain distribution of H''-1-15 specimen.

## V. Conclusion

Based on the experimental results, the following conclusion can be drawn:

- From the tests results It was found that the bonded length have an effect on the bond strength of CFRP sheet attached to concrete surface where, the PC and PU in normal strength concrete was increased up to bonded length of 150mm whilst, in high strength concrete the effect was extended to bond length of 300mm.

- The effective bonded length is defined as the length of sheet that contributes to the bond strength and the ultimate load, so the effective bonded length in NSC was found 150mm whilst in HSC was started from 220mm where the failure mode altered from peeling to rupture of CFRP sheet.
- The stiffness and the ultimate capacity of the beams increased due to increasing the CFRP sheet width and the roughness of concrete surface in both NSC and HSC groups. The increase in PU was about 50%, 67% due to increase in the sheet width and 12.5%, 25% due to surface roughness for NSC and HSC, respectively. The ultimate deflection,  $\Delta_U$ , was decreased with about 13% due to increasing the fiber width in HSC.
- The increase in number of plies (stiffness) of CFRP sheet had a remarkable effect, where the beams experienced a brittle failure mechanism, however in this case sudden debonding of the CFRP sheet from the concrete surface occurred without concrete splitting. The cracking load and ultimate capacity of the beam increased by 33% and 20% only (which was not proportional to the number of plies) for beam with bonded length of 150mm. In addition, a reduction in the ultimate deflection (22%, 27% for  $L_b=150\text{mm}$ , 220mm, respectively) which indicating that the addition of CFRP layers greatly reduces the deformability of the beam at ultimate stage of loading.
- The bond length affects significantly the average bond stress of the strengthened beams (shear bonding stress due to flexural loading). With increasing the bond length from 100mm to 220mm the average bonding stress on the CFRP sheet reduced with about 55% in NSC. Whilst, The reduction was about 38% with increasing the bond length from 100mm to 220mm and was about 60% with increasing  $L_b$  from 100mm to 300mm in HSC. The bond width of CFRP sheet was significantly influenced the bond stress on the fiber. Due to doubling the width of CFRP sheet from 50mm to 100mm, the average bond stress reduced by about 55%.
- The strain distribution shows almost linear behaviour when the applied load was close to ultimate load relatively in all cases. The maximum strain in NSC specimens was higher in comparison with HSC specimens. The effect of bonded length on the maximum strain value was appeared only in NSC specimens, with increasing the bonded length the ultimate strain value increased.
- The strengthening material types also affect the bond between fiber and concrete. Usage of glass fibre type or combinations of externally bonded composite of Glass and Carbon Fiber Reinforced Polymer (GFRP/CFRP) sheet in strengthening the beams in flexure needs to be examined in future. Usage of such these materials

expected to provide better performance with a suitable improvement in strength and ductility of the beam in flexure, furthermore with lower in cost in comparison with CFRP sheet only.

## REFERENCES

- [1] H. Toutanji, L. Zhao, Y. Zhang, "Flexural behavior of reinforced concrete beams externally strengthened with CFRP sheets bonded with an inorganic matrix", *Engineering Structures* 28, pp. 557–566, 2006.
- [2] B. Miller, and A. Nanni, "Bond Between CFRP Sheets and Concrete", *Proceedings, ASCE 5th Materials Congress, Cincinnati, OH, L.C. Bank, Editor, May 10-12, pp. 240-247, 1999.*
- [3] L. De Lorenzis, B. Miller, and A. Nanni, "Bond of Fiber-Reinforced Polymer Laminates to Concrete", *ACI Materials Journal*, V. 98, No. 3, pp. 256-264, May-June 2001.
- [4] S.Y. Seo, L. Feo, D. Hui, "Bond strength of near surface-mounted FRP plate for retrofit of concrete structures", *Composite Structures*, V. 95, pp. 719–727, 2013.
- [5] R. A. Hawileh, H. A. Rasheed, J. A. Abdalla, A. K. Al-Tamimi, "Behavior of reinforced concrete beams strengthened with externally bonded hybrid fiber reinforced polymer systems", *Materials and Design*, V. 53, pp. 972-982, 2014.
- [6] A. Morsy, E. T. Mahmoud, "Bonding techniques for flexural strengthening of R.C. beams using CFRP laminates", *Ain Shams Engineering Journal*, V. 4, pp. 369–374, 2013.
- [7] M. Ekenel, V. Stephen, J.J. Myers, R. Zoughi, "Microwave NDE of RC Beams Strengthened with CFRP Laminates Containing Surface Defects and Tested Under Cyclic Loading", *Electrical and Computer Engineering, University of Missouri-Rolla, Rolla, MO 65409, USA*, pp 1-8, 2004.
- [8] F. Ceroni, "Experimental performances of RC beams strengthened with FRP materials", *Construction and Building Materials*, V. 24: pp. 1547-59, 2010.
- [9] Y.C. Wang, K. Hsu, "Design recommendations for the strengthening of reinforced concrete beams with externally bonded composite plates", *Composite Structures*, V. 88, pp. 323-32, 2009.
- [10] F. Ceroni, M. Pecce, S. Matthys, L. Taerwe, "Debonding strength and anchorage devices for reinforced concrete elements strengthened with FRP sheets", *Composites Part B: Engineering*. 39: 429-41, 2008.
- [11] G.J. Xiong, X. Jiang, J.W. Liu, L. Chen "A way for preventing tension delamination of concrete cover in midspan of FRP strengthened beams", *Construction and Building Materials*. 21: 402-8, 2007.
- [12] I.G. Costa, B. Jao, "Flexural and shear strengthening of RC beams with composite materials - The influence of cutting steel stirrups to install CFRP strips", *Cement and Concrete Composites*. In Press, Corrected Proof, 2010.
- [13] L. Ombres, "Prediction of intermediate crack debonding failure in FRP-strengthened reinforced concrete beams", *Composite Structures*. V. 92, pp. 322-9, 2010.
- [14] H. Pham, R. Al-Mahaidi, "Prediction models for debonding failure loads of carbon fiber reinforced polymer retrofitted reinforced concrete beams", *J Compos Constr, ASCE*, V.10, pp. 48-59, 2006.
- [15] N. Attari, S. Amziane, M. Chemrouk, "Flexural strengthening of concrete beams using CFRP, GFRP and hybrid FRP sheets", *Construction and Building Materials*, V. 37, pp. 746–757, 2012.
- [16] B. D. Millre, "Bond Between Carbon Fiber Reinforced Polymer Sheets and Concrete", *Msc Thesis, Center for Infrastructure Engineering Studies (CIES), University of Missouri-Rolla, 1999.*
- [17] E.Y. Sayed-Ahmed, R. Bakay, N.G. Shrive, "Bond Strength of FRP Laminates to Concrete: State-of-the-Art Review", *Electronic Journal of Structural Engineering*, V.9, pp. 45-61, 2009.
- [18] N. Aravind, Amiya K. Samanta, Dilip Kr. Singha Roy, and Joseph V. Thanikal, "Flexural strengthening of Reinforced Concrete (RC) Beams Retrofitted with Corrugated Glass Fiber Reinforced Polymer (GFRP) Laminates", *Curved and Layer. Struct.*, V. 2:244–253, 2015.
- [19] D. U. Choi, T. H. K. Kang, S. S. Ha, K. H. Kim, and W. Kim, "Flexural and bond behavior of concrete beam strengthened with hybrid carbon-glass fiber reinforced polymer sheet", *ACI Struct. J.*, vol. 108, no. 1, pp. 90-98, 2011.
- [20] R. Djamaluddin, M. A. Sultan, R. Irmawati, and H. Shinichi, "Bond Characteristics of GFRP Sheet on Strengthened Concrete Beams due to Flexural Loading", *IACSIT International Journal of Engineering and Technology*, Vol. 7, No. 2, April 2015.

## AUTHOR'S PROFILE

**Dr. Magda I. MOUSA** is currently Associate Professor in Civil Engineering at El-Mansoura University, Egypt. She is having experience of more than 30 yrs in teaching at both undergraduate and postgraduate level, research and structural designing and construction supervision. She has done her B.Sc (Civil Eng.) and M.Sc (Structural Eng.) from El-Mansoura University and completed her doctorate (PhD) from IIT Madras, India. She has published many research papers in national and international journals and conferences. She has candidates which completed for MSc and PhD and others still working.